Heat Capacity, Alternating Current Magnetic Susceptibilities, and Pressure Effect for the Cyano-Bridged Bimetallic Ferromagnet $Mn_2(H_2O)_5Mo(CN)_7 \cdot 4H_2O$ (α Phase)

Joulia Larionova,[†] Olivier Kahn,*[,†] Juan Bartolome,*[,‡] Ramon Burriel,[‡] Miguel Castro,[‡] Vadim Ksenofontov,[§] and Philipp Gütlich*[,§]

Laboratoire des Sciences Moléculaires, Institut de Chimie de la Matière Condensée de Bordeaux, UPR CNRS No 9048, 33608 Pessac, France, Instituto de Ciencia de Materiales de Aragon, CSIS-Universidad de Zaragoza, 50009 Zaragoza, Spain, and Institut für Anorganische Chemie und Analytische Chemie, Universität Mainz, 55099 Mainz, Germany

Received August 9, 1999

The goal of this paper is to obtain further information on the magnetic phase diagram of the cyano-bridged bimetallic ferromagnet of formula $Mn_2(H_2O)_5Mo(CN)_7 \cdot 4H_2O$ (α phase). For that, the temperature dependence of the heat capacity has been measured. A λ peak has been observed at $T_c = 50.5$ K, corresponding to the transition between the ferromagnetic and paramagnetic states. The temperature dependencies of the alternating current (ac) in-phase and out-of-phase magnetic susceptibilities have also been measured on single crystals oriented along their magnetic axes, *a*, *b*, and *c**. The effect of the frequency and of the value of the static field have been investigated. These data confirm the magnetic phase diagram determined previously from single-crystal direct current (dc) magnetic measurements. The effect of pressure on the magnetic properties has also been investigated. T_c was found to vary linearly as a function of pressure, with a positive dT_c/dP slope. All these results have been discussed.

Introduction

Recently, we described the structure and the magnetic properties of a cyano-bridged bimetallic compound of formula $Mn_2(H_2O)_5Mo(CN)_7 \cdot 4H_2O$ (α phase).[1] This compound crystallizes in the space group $P2_1/c$ and has a three-dimensional structure. This structure consists of ladders made of edge-sharing lozenge motifs ($MoCN$-$MnNC)_2$ running along the *a* direction. These ladders are linked further along the *b* and *c* directions. The structure as a whole viewed along the *a* direction is recalled in Figure 1. This structure is totally different of that of the Prussian blue like phases which are faced-centered cubic[2−8] and, owing to its low symmetry, leads to very interesting anisotropy properties which had not thus far been observed for molecule-based magnetic materials.

Both temperature dependencies of the magnetic susceptibility and field dependencies of the magnetization in the direct current (dc) mode have been investigated along the three magnetic axes, *a*, *b*, and *c**. These single-crystal magnetic measurements revealed that the com-

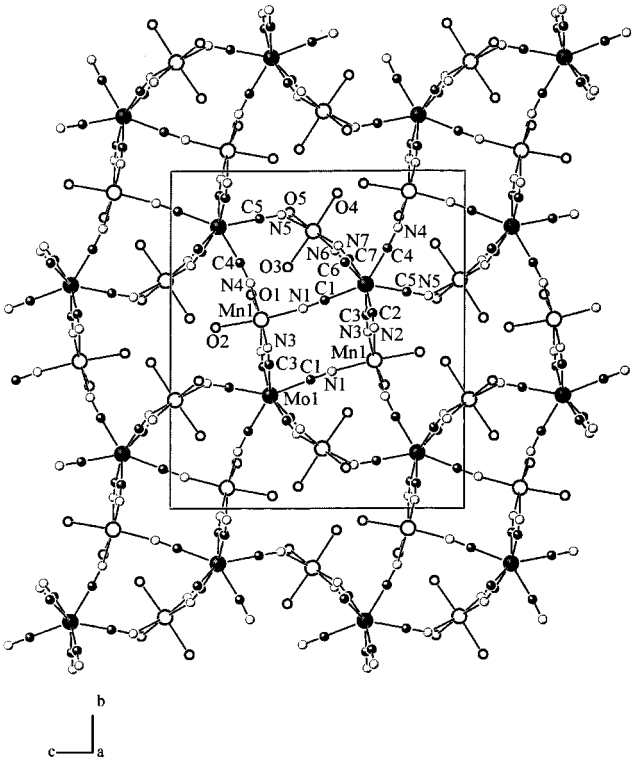

Figure 1. Structure of $Mn_2(H_2O)_5Mo(CN)_7 \cdot 4H_2O$ (α phase) viewed along the *a* axis.

[†] Institut de Chimie de la Matière Condensée de Bordeaux.
[‡] CSIS-Universidad de Zaragoza.
[§] Universität Mainz.

(1) Larionova, J.; Clérac, R.; Sanchiz, J.; Kahn, O.; Gohlen, S.; Ouahab, L. *J. Am. Chem. Soc.* **1998**, *120*, 13088.
(2) Ludi, A.; Güdel, H. U. *Struct. Bonding (Berlin)* **1973**, *14*, 1.
(3) Kahn, O. *Adv. Inorg. Chem.* **1995**, *43*, 179.
(4) Babel, D. *Comments Inorg. Chem.* **1986**, *5*, 285.
(5) Gadet, V.; Mallah, T.; Castro, I.; Verdaguer, M. *J. Am. Chem. Soc.* **1992**, *114*, 9213.
(6) Mallah, T.; Thiébaut, S.; Verdaguer, M.; Veillet, P. *Science* **1993**, *262*, 1554.
(7) Entley, W. R.; Treadway, C. R.; Girolami, G. S. *Mol. Crys. Liq. Cryst.* **1994**, *273*, 153.
(8) Entley, W. R.; Girolami, G. S. *Science* **1995**, *268*, 397.

10.1021/cm991117t CCC: $18.00 © 1999 American Chemical Society
Published on Web 10/27/1999

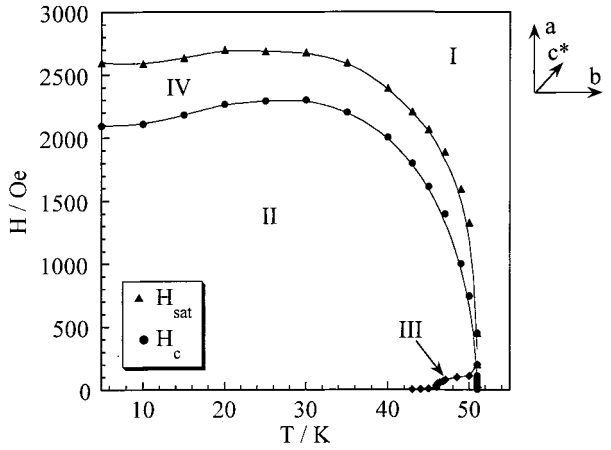

Figure 2. Magnetic phase diagram for $Mn_2(H_2O)_5Mo(CN)_7 \cdot 4H_2O$ (α phase). The full lines are just eye guides.

pound is a three-dimensional ferromagnet, with T_c estimated as 51 K, without hysteresis effect. Two additional magnetic phenomena were detected, namely: (i) in zero field, another transition occurs, at 43 K, which disappears when applying a field higher than 100 Oe; (ii) the 2-fold *b* axis of the monoclinic lattice is the easy magnetization axis, but when the field is applied along the *a* axis a spin reorientation phenomenon occurs,[9−13] and the *ab* plane becomes almost isotropic. From the single-crystal magnetic data, it has been possible to determine the magnetic phase for a field applied along *a*. This diagram, shown in Figure 2, presents four domains. I is the paramagnetic domain; II and III are two ferromagnetically ordered domains; IV is a spin reorientation domain. The difference between domains II and III are unknown. Only accurate neutron diffraction experiments could specify the exact nature of each of them.

The goal of this paper is to obtain additional insights on the magnetic structure of the compound from alternating current (ac) magnetic measurements, and to see whether these new magnetic data confirm or refute the magnetic phase diagram of Figure 2. We will also present the temperature dependence of the heat capacity, which can provide definite proof of the existence of long-range order in a magnetic transition. As a matter of fact, in a para-ferromagnetic transition, such as the one with which we are dealing, a sharp peak should appear at the transition temperature T_c. Finally, we will report on the pressure dependence of the critical temperature.

Experimental Section

Synthesis. Well-shaped single crystals of $Mn_2(H_2O)_5Mo(CN)_7 \cdot 4H_2O$ (α phase) were obtained as previously described by slow diffusion of aqueous solutions containing $K_4[Mo(CN)_7] \cdot 2H_2O$ and $[Mn(H_2O)_6](NO_3)_2$, respectively.[1] The crystals have the shape of plates. The *a*, *b*, and *c* crystallographic axes correspond to the long, intermediate, and small edges, respectively.

Heat Capacity Measurements. These were performed using a Sinku-Riku ACC-1VL ac calorimeter between 4.2 and 300 K. The sample was a single-crystal slab of around 0.5 × 0.5 × 0.1 mm^3 with the *c* crystal axis perpendicular to the larger surface of the parallelepiped. The frequency used for the excitation signal was between 2 and 15 Hz. Scan rates between 10 and 30 K per hour were used in the measurements with the smaller values at low temperatures and through the transition. Several runs on heating and cooling were performed to study the existence of thermal hysteresis. This technique provides relative heat capacity data that in principle can be scaled with the aid of an absolute measurement at room temperature taken with DSC technique.

Alternating Current Magnetic Measurements. These were carried out with a Quantum Design MPMS-5S SQUID magnetometer working in both dc and ac mode down to 2 K and up to 50 kOe.

Pressure Study. The temperature dependence of the magnetization under pressure was measured with a Foner-type magnetometer PAR 151 in the 4.4−80 K temperature range, using a laboratory-made high-pressure cell.[14,15] The pressure-transmitting medium was a silicon oil. The cell had the following characteristics: weight, 8 g; range of pressure, 0.5−13 kbar; accuracy, 0.25 kbar; the nonhydrostaticity is less than 0.5 kbar. The sample holder is cylindrically shaped; its dimensions are 1 mm in diameter and 5−7 mm in length. The pressure was calibrated using the transmission temperature of superconductivity tin of purity 0.9999. The sample consisted of a collection of single crystals oriented along the *a* axis, and the magnetic field was applied perpendicular to this axis. The measurements were performed at fixed pressures up to 8.5 kbar. The applied magnetic field was 1 Oe.

Results

Temperature Dependence of the Heat Capacity. The C_p versus T curve is shown in Figure 3 (top). This curve exhibits a well-pronounced λ anomaly, typical for a magnetic order−disorder transition, in addition to the lattice contribution. The transition temperature is found as $T_c = 50.5$ K. No hysteresis effect was observed. The synthetic process affords a β phase in addition to the α phase to which this paper is devoted, and so far we have not been able to obtain more than a few single crystals of this α phase. As a consequence, we could not perform DSC measurements to establish the absolute scale of the heat capacity. A tentative evaluation of the lattice contribution as a polynomial of order 5 allowed us to extract the magnetic anomalous contribution, albeit in arbitrary unit, as shown in Figure 3 (bottom). Therefore, the entropy variation associated with the transition at 50.5 K has not been determined. In other respects, no anomalous contribution could be detected at 43 K.

Temperature Dependencies of the Alternating Current Susceptibilities in a Zero Static Field. The temperature dependencies of the ac susceptibility were measured in zero field and with a frequency of 125 Hz along the three magnetic axes, *a*, *b*, and *c**. The results for the in-phase response, χ'_M, are shown in Figure 4. The curves along the *b* and *c** axes are rather similar. As the temperature is lowered, χ'_M increases abruptly below ∼52 K. The critical temperature, $T_c = 50.5$ K, corresponds to an inflection point of the χ'_M versus T curve. Between 50.5 and 43 K, χ'_M remains constant, then shows an anomaly at 43 K, and eventually de-

(9) Salgueiro da Siva, M. A.; Moreira, J. M.; Mendes, J. A.; Amaral, V. S.; Sousa, J. B.; Palmer, S. B. *J. Phys.: Condens. Mater.* **1995**, *7*, 9853.
(10) Asti, G.; Bolzoni, F. *J. Magn. Magn. Mater.* **1980**, *20*, 29.
(11) Mendoza, W. A.; Shaheen, S. A. *J. Appl. Phys.* **1996**, *79*, 6327.
(12) Cao, G.; McCall, S.; Crow, J. E. *Phys. Rev. B* **1997**, *55*, R672.
(13) Kou, X. C.; Dahlgren, M.; Grössinger, R.; Wiesinger, G. *J. Appl. Phys.* **1997**, *81*, 4428.
(14) Baran, M. *Physica C* **1996**, *261*, 125.
(15) Baran, M.; Dyakonov, V.; Gladczuk, L.; Levchenko, G.; Piechota, S.; Szymzak, H. *Physica C* **1985**, *241*, 383.

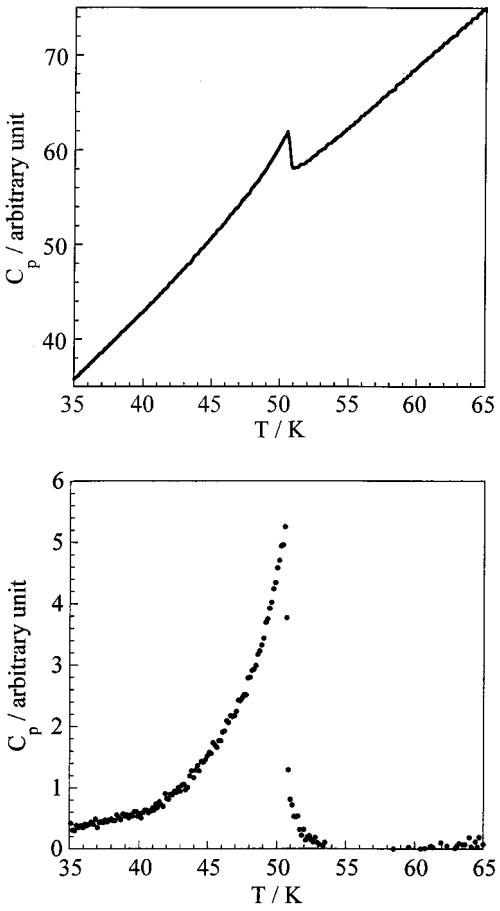

Figure 3. (top) Temperature dependence of the heat capacity for $Mn_2(H_2O)_5Mo(CN)_7 \cdot 4H_2O$ (α phase) and (bottom) magnetic anomalous contribution (see text).

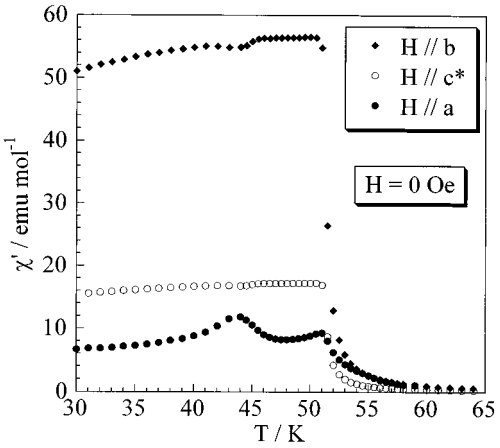

Figure 4. Temperature dependencies of the in-phase ac susceptibility, χ'_M, in a zero static field along the *a*, *b*, and *c** magnetic axes.

creases smoothly as *T* is lowered further. Along the *a* axis, χ'_M exhibits two maxima, at 50.5 and 43 K, and decreases smoothly as *T* is lowered below 40 K. The compound is strongly anisotropic. As a matter of fact, χ'_M is roughly seven times as large along the *b* axis as along the *a* axis.

The temperature dependencies of the out-of-phase response, χ''_M, are shown in Figure 5. Along the three magnetic axes, χ''_M is zero down to 51 K, increases slightly as *T* is lowered below 51 K, and then exhibits a peak at 43 K. As *T* is lowered below ~40 K, χ''_M

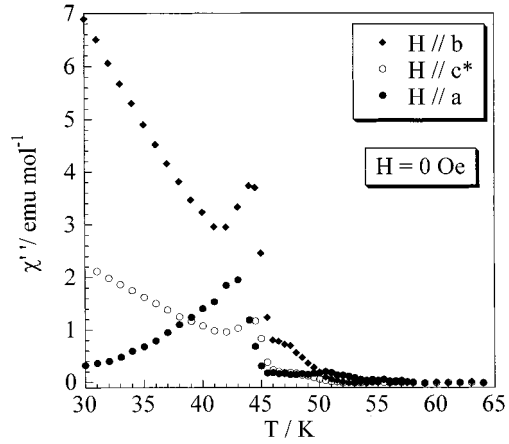

Figure 5. Temperature dependencies of the out-of-phase ac susceptibily, χ''_M, along the *a*, *b*, and *c** magnetic axes.

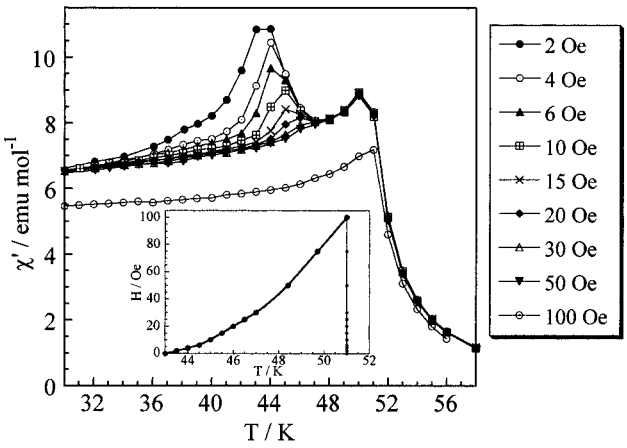

Figure 6. Temperature dependencies of the in-phase ac magnetic susceptibility, χ'_M, for different values of the applied static field up to 100 Oe along the *a* axis.

increases again along the *b* and *c** axes, and decreases along the *a* axis.

The effect of the frequency of the oscillating field was investigated for an oscillating field applied along the *a* axis. The peak at 50.5 K is not at all modified while the peak at 43 K is shifted to 44 K as the frequency is increased from 1 to 999 Hz. This behavior confirms that the transition at 50.5 K is a normal transition between a paramagnetic and a magnetically ordered state and that the transition at 43 K is of another nature, occurring most likely between two magnetically ordered states.

Temperature Dependencies of the Alternating Current Susceptibilities under a Static Field. The magnetic data reported so far were obtained in a zero static field. The temperature dependencies of χ'_M and χ''_M were also measured for several values of the static field. The χ'_M versus *T* curves for a static field between 2 and 100 Oe applied along the *a* axis are represented in Figure 6. The frequency is maintained at 125 Hz. The transition temperature observed at 43 K in zero static field is shifted toward higher temperatures as the static field increases, and eventually merges with the transition at 50.5 K for a field value of ~100 Oe. Conversely, the transition temperature at 50.5 K is not influenced by the field. The temperature dependence of the field for which the two transitions are observed, deduced from these experiments, are represented in the insert of

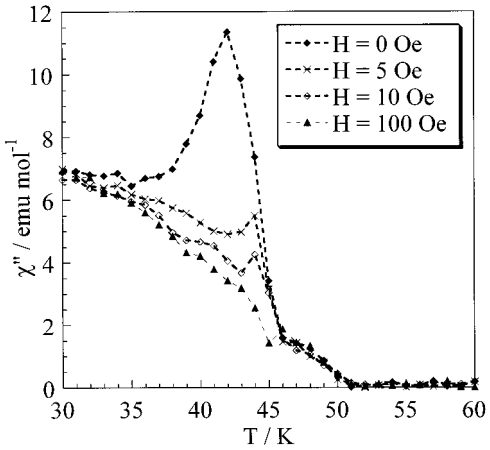

Figure 7. Temperature dependencies of the out-of-phase ac magnetic susceptibility, χ''_M, for different values of the applied static field up to 100 Oe along the *b* axis.

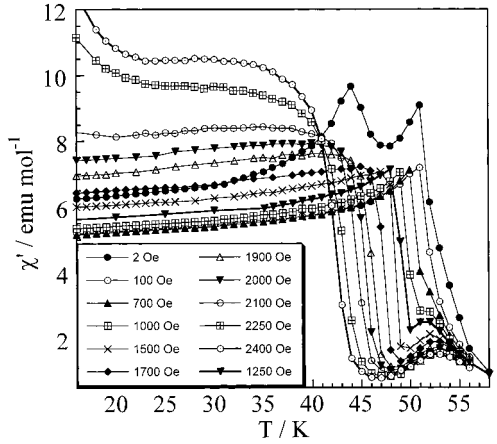

Figure 8. Temperature dependencies of the in-phase ac magnetic susceptibility, χ''_M, for different values of the applied static field up to 2400 Oe along the *a* axis.

Figure 6. The anomaly at 43 K is less pronounced on the $\chi'_M = f(T)$ curves along the *b* and *c** axes. However, the same $H = f(T)$ curves as that of Figure 6 (insert) could be deduced from the $\chi'_M = f(T)$ curves along those two axes. These $H = f(T)$ curves can be also deduced from the $\chi''_M = f(T)$ curves. For instance, Figure 7 shows the temperatures dependencies of χ''_M for various values of the static field applied along the *b* axis. The intensity of the peak at 43 K diminishes as the field increases and disappears for a field of ~100 Oe.

A field-induced spin reorientation phenomenon along the *a* axis has been characterized through dc magnetic measurements. To try to obtain further insights on this phenomenon, the χ'_M versus *T* curves along this direction were also measured when increasing the static field up to the saturation field value. The results are shown in Figure 8. The behavior as the field increases from zero up to 100 Oe was discussed above. Under 100 Oe, a single peak is observed at 50.5 K. Increasing further the field results in the appearance of a second peak below 50.5 K. This peak is shifted toward lower temperatures as the field increases. When the field is larger than 2100 Oe, a third peak appears at even lower temperatures. This behavior is perfectly in line with the magnetic phase diagram recalled in Figure 2. Under 100 Oe, there is a single magnetic transition at 50.5 K. For field values between 100 and 2100 Oe, two boundaries

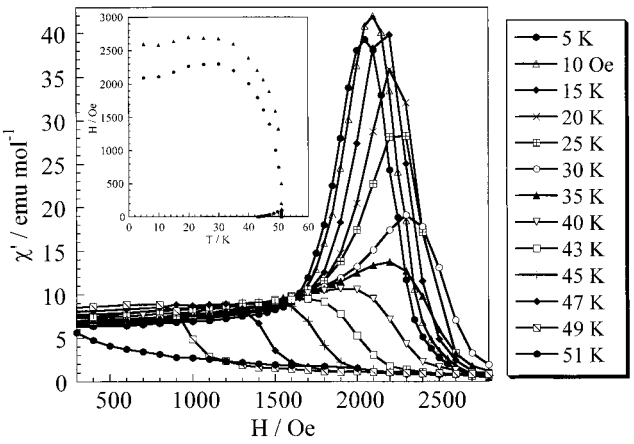

Figure 9. Field dependencies of the in-phase ac magnetic susceptibility, χ'_M, at different temperatures between 5 and 51 K. The static field is applied along the *a* axis. The insert shows the magnetic phase diagram deduced from this experiment (see text).

of the magnetic phase diagram are crossed, between domains IV and I around 50.5 K, and between domains II and IV at lower temperatures. For field values between 2100 and 2300 Oe, the boundary between domains IV and I is crossed once, but the boundary between domains II and IV is crossed twice.

Quite interestingly, from the curves of Figure 8, it is possible to plot the H_c and H_{sat} versus *T* curves, where H_c is the critical field and H_{sat} the saturation field of the spin reorientation phenomenon; H_c is determined as the field for which χ'_M is maximum, and H_{sat} as the field for which the χ'_M versus *H* curve presents an inflection point. Adding the $H = f(T)$ curve of Figure 6 (insert) results in a magnetic phase diagram strictly identical to that displayed in Figure 2.

Field Dependencies of the Alternating Current Magnetic Susceptibilities. Figure 9 shows the field dependencies of χ'_M along the *a* axis at different temperatures between 5 and 51 K. χ'_M remains almost constant in low field and then increases rapidly as the field approaches the critical value of the spin reorientation phenomenon, reaches a maximum for this value of the critical field, H_c, and then decreases with an inflection point for the value of the saturation field, H_{sat}, and eventually tends to zero. As the temperature increases, the maximum value of χ'_M decreases, as well as the field H_c for which this maximum value is observed. For each χ'_M versus *H* curve, it is possible to deduce the H_c and H_{sat} values at a given temperature and then to rebuild again the magnetic phase diagram of Figure 2, as shown in the insert of Figure 9.

Pressure Effect. The temperature dependencies of the magnetization normalized at the saturation magnetization, M/M_{sat}, under various pressures, *P*, are shown in Figure 10. As the pressure increases, the magnetization curve is shifted practically parallel toward higher temperatures, and the critical temperature increases from 50.5 K under ambient pressure up to 55.5 K under 8.5 kbar. This pressure dependence of T_c, shown in the insert of Figure 10, is practically linear. The slope dT/dP may be estimated as $+0.59$ K kbar^{-1}.

Discussion

The temperature dependence of the heat capacity confirms the magnetic data as far as the transition at

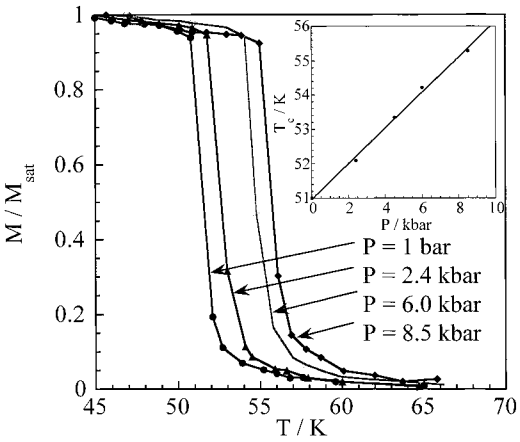

Figure 10. Temperature dependencies of the normalized magnetization under various pressures. The insert shows the pressure dependence of the critical temperature.

50.5 K is concerned and improves the accuracy on the T_c value. The largest entropy variation is associated with this order−disorder magnetic transition. The fact that no hysteresis was observed agrees with the fact that the transition between ferromagnetic and paramagnetic states is of the second order.

The heat capacity curve does not detect the second transition, occurring at 43 K in zero field. Therefore, the entropy change associated with this 43 K transition is very weak. This transition occurs between two ferromagnetically ordered states.[16−18] These two states are most likely very close to each other. It has been suggested that they might differ by the degree of canting. Alternatively, one of the two states might be a pure ferromagnetic state with the magnetic moments strictly aligned along the *b* axis in zero field and the other state might be very weakly canted.

Let us now examine what information is provided by the ac magnetic measurements. The ac magnetic susceptibility is determined from its two components, the in-phase, or real, component, χ'_M, and the out-of-phase, or imaginary, component, χ''_M. χ'_M [$= (dM/dH)_{H=H_0}$ where H_0 is the static field] is an initial susceptibility with the same phase as the oscillating field. χ''_M characterizes the phase delay of the magnetization with respect to the oscillating field. This phase delay is due to the energy loss arising from the displacement of the domain walls.[16]

We have seen that the ac response is much stronger along *b* than along *a* and *c**. The two main contributions to the ac magnetic susceptibility are the displacement of the domain walls and the rotation of the magnetic moments.[19,20] When the field is applied along the easy magnetization axis, *b* in our case, both contributions are present. On the other hand, when the field is applied perpendicularly to the easy magnetization axis, only the rotation of the magnetic moments contributes to the ac response. The very high response along *b* as compared to the responses along *a* and *c** indicates that the domain walls move almost freely.

The most interesting information is provided by the ac measurements under a static field. These measurements perfectly confirm the magnetic phase diagram determined from the dc measurements. Two phenomena occur in addition to the long-range ferromagnetic ordering at 50.5 K. First, there are two magnetically ordered domains, one of them, noted domain III, being limited to the 43−50.5 K temperature range and 0−100 Oe field range. The transition between these two domains, at 43 K in zero field, is accompanied by a well-marked peak in the $\chi'_M = f(T)$ curve along the *a* axis, and only by a weakly pronounced break along the other two magnetic axes. This strongly suggests that the main difference between the domains II and III concerns the component of the resulting moment along *a*. Assuming that the magnetic symmetry of the low-temperature domain II is lower than that of the high-temperature domain III, we may assume that domain III is a perfectly ferromagnetic domain with the magnetic moments aligned along *b* in zero field and that a small canting occurs as *T* is lowered below 43 K, with a weak component of the resulting moment along *a*.[21,22] If it was so, applying a field of 100 Oe along *a* would destabilize the perfectly ferromagnetic domain in favor of the weakly canted domain. Alternatively, the two domains are weakly canted, with a component of the moment along *a*, the degree of canting being slightly more pronounced in domain II.

The second unexpected phenomenon is the field-induced spin reorientation when the field is applied along *a*. This phenomenon is related to the presence of an inflection point in the field dependence of the magnetization along this direction. In zero field, the moment is essentially aligned along *b*. When applying the field, first it hardly rotates from *b* to *a*, and then for a critical value of the field the rotation becomes much easier. Finally, for a saturation value of the field, the moment is aligned along *a*.

The pressure study brings some new insights on the magnetic properties of the compound. T_c was found to vary linearly with *P*, with a positive dT_c/dP slope. The observed increase of T_c under pressure is not a general phenomenon. If we restrict ourselves to molecular-based ferromagnets, both positive and negative dT_c/dP values were reported. dT_c/dP was found to be positive for NH_4-Ni(mnt), with $dT_c/dP = 0.4$ K kbar^{-1},[23] as well as for [Fe(Cp*)$_2$][TCNE], with $dT_c/dP = O.22$ K kbar^{-1}.[24] dT_c/dP was also reported to be weakly positive for the β phase of magnesium(II) phthalocyanine which is a canted ferromagnet.[25] On the other hand, dT_c/dP was found to be negative for the β phase of *p*-nitrophenyl-nitronyl-nitroxide, with $dT_c/dP = -0.034$ K kbar^{-1},[26] and for TDAE-C_{60}, with dT_c/dP close to -10 K kbar^{-1}

(16) Palacio, F.; Lazaro, F. J.; van Duyneveldt, J. *Mol. Cryst. Liq. Cryst.* **1989**, *176*, 289.
(17) Takeda, K.; Awaga, K. *Phys. Rev. B* **1997**, *56*, 14560.
(18) Süllow, S.; Nieuwenhuys, G. J.; Menovsky, A. A.; Mydosh, J. A.; Mentink, S. A. M.; Mason, T. E.; Buyers, W. J. L. *Phys. Rev. Lett.* **1997**, *78*, 354.
(19) Chikazumi, S. *Physics of Magnetism*; Krieger: Malabar, 1978.
(20) Rillo, C.; Chaboy, J.; Navarro, R.; Bartolomé, J.; Fruchart, B.; Chenevrier, B.; Yaouanc, A.; Sagawa, M.; Hirosawa, S. *J. Appl. Phys.* **1988**, *64*, 5534.
(21) Dzialoshinsky, I. *J. Phys. Chem. Solids* **1958**, *4*, 241.
(22) Moriya, T. *Phys. Rev.* **1960**, *120*, 91.
(23) Coomer, A. T.; Beljonne, B.; Friend, R. H.; Bredas, J. L.; Charlton, A.; Robertson, N.; Underhill, A. E.; Kurmoo, M,; Day, P. *Nature* **1996**, *380*, 144.
(24) Huang, Z. J.; Cheng, F.; Ren, Y. T.; Xue, Y. Y.; Chu, C. W.; Miller, J. S. *Appl. Phys.* **1993**, *73*, 6563.
(25) Awaga, K.; Maruyama, Y. *Phys. Rev. B* **1991**, *44*, 2589.
(26) Takeda, K.; Konishi, K.; Tamura, M.; Kinoshita, M. *Mol. Cryst. Liq. Cryst.* **1995**, *273*, 57.

K.[27] A negative dT_c/dP plot was also observed for layered compounds.[28] Such negative dT_c/dP values are usually interpreted as resulting from a competition between ferro- (F) and antiferromagnetic (AF) interactions. At ambient pressure, the F interactions dominate, and the material exhibits a long-range ferromagnetic ordering. Under pressure, the AF interactions are more enhanced than the F ones, and the critical temperature diminishes. Such a situation does not occur for the title compound; competing interactions do not occur in the studied range of pressure. Applying pressure results in a decrease of the bond lengths along the $Mo^{III}-C-N-Mn^{II}$ linkages, and in a corresponding increase of the F interactions. It is worthwhile to stress that such a behavior is in line with the spin−polarization mechanism suggested for the F interaction between low-spin Mo^{III} and high-spin Mn^{II} through the cyano bridge.[29] As a matter of fact, when the bond lengths are shortened, the negative spin densities along the Mo−C−N directions of the $Mo(CN)_7$ fragment are enhanced, as well as the interactions between these negative spin densities and the σ singly occupied orbitals of Mn^{II}.

Conclusion

A this stage, we would like to sum up what is known and well understood concerning the title compound and what needs to be investigated and/or interpreted further.

$Mn_2(H_2O)_5Mo(CN)_7 \cdot 4H_2O$ (α phase) is the first three-dimensional cyano-bridged magnet whose structure has been solved accurately. It is also the first compound of this family whose magnetic phase diagram has been determined from single-crystal magnetic measurements, both in the dc and ac mode. The compound is a ferromagnet. Applying pressure results in an enhancement of the ferromagnetic interaction, probably due to a shortening of the bond lengths. No competing effect between F and AF interactions is observed. The ferromagnetic nature of the interaction along the $Mo^{III}-C-N-Mn^{II}$ linkage has been attributed to a spin polarization effect.[29] This hypothesis deserves to be substantiated by theoretical calculations, using for instance the DFT formalism.[30,31] Moreover, it would be interesting to see to what extent the dipolar effects involving the $S_{Mn} = {}^5/_2$ spins of the Mn^{II} sites do also contribute to the parallel alignment of he local spins.

The magnetic phase diagram reveals the presence of two ferromagnetically ordered domains, and the transition between these two domains occurs with a very weak entropy variation, not detected on the temperature dependence of the heat capacity. Neutron diffraction experiments are in progress to characterize the difference between these two ferromagnetic domains. It has been suggested that they could differ by a degree of canting. In the ferromagnetic domains, the compound is strongly anisotropic, with the easy magnetization axis along the 2-fold rotation axis, *b*, of the lattice. This anisotropy may arise from both the anisotropy of the local **g** tensor for the $[Mo^{III}(CN)_7]$ chromophore and the dipolar interactions. Again, the exact role of the dipolar interactions needs to be specified.

The magnetic phase diagram also reveals the occurrence of a spin reorientation phenomenon when the field is aligned along the *a* axis, i.e., the axis of the ladders forming the structure. To the best of our knowledge, this phenomenon has thus far not been observed in magnetic molecular materials and is very scarce for insulating magnets. It might also be due to a competition between dipolar interactions and anisotropy of the **g** tensor for $[Mo(CN)_7]$. In zero field, the ferromagnetically coupled local spins would tend to align along the direction of the Mo−C−N−Mn−N−C infinite linkages, i.e., the *b* axis, which minimizes the dipolar energy.[32] When the magnetic field reaches a certain value, the **g** anisotropy for Mo^{III} would favor the spin alignment along another direction.

In a near future, we hope to be able to characterize further the magnetic behavior of this ferromagnet synthesized from a molecular precursor, using other physical techniques such as single-crystal EPR and neutron diffraction.

Acknowledgment. This work was partly funded by the TMR Research Network ERBFMRXCT980181 of the European Union, entitled “Molecular Magnetism; from Materials toward Devices”. P.G. acknowledges financial support from the Deutsche Forschungs Gemeinschaft, the Fonds der chemischen Industrie, and the University of Mainz (MWFZ).

CM991117T

(27) Thompson, J. D.; Sparn, G.; Dierdrich, F.; Grüner, G.; Holczer, K.; Kaner, R. B.; Whetten, R. L.; Allemand, P. M.; Wudl, F. *Mater. Res. Soc. Symp.* **1992**, *247*, 315.

(28) Levchenko, G.; Ksenofontov, V.; Dulnev, V.; Zubov, E.; Rabu, P.; Drillon, M.; Gütlich, P. Unpublished results.

(29) Kahn, O.; Larionova, J.; Ouahab, L. *Chem. Commun.* **1999**, 945.

(30) Ruiz, E.; Alemany, P.; Alvarez, S.; Cano, J. *Inorg. Chem.* **1997**, *36*, 3683; *J. Am. Chem. Soc.* **1997**, *119*, 1297.

(31) Baron, V.; Gillon, B.; Cousson, A.; Mathonière, C.; Kahn, O.; Grand, A.; Öhrström, L.; Delley, B.; Bonnet, M.; Boucherle, J. X. *J. Am. Chem. Soc.* **1997**, *119*, 3500.

(32) Caneschi, A.; Gatteschi, D.; Renard, J. P.; Rey, P.; Sessoli, R. *Inorg. Chem.* **1989**, *28*, 3314.